

Model-Based Optimization of Hydrogen Storage for Military Ground Vehicle Applications

Ben Paczkowski¹, Andrew Wiegand²

¹US Army DEVCOM GVSC, Warren, MI

²PM Self-Propelled Howitzer Systems, Warren, MI

ABSTRACT

As the Army begins to explore the electrification of its ground vehicle fleet, several technologies are of interest to help clear the large hurdle presented by vehicles' energy needs. Hydrogen fuel cells have potential as a solution to this problem but there are many challenges that need to be addressed, such as hydrogen storage. Siemens LMS Amesim was used to simulate the performance of several wheeled and tracked vehicles in order to evaluate several hydrogen storage methods and materials to determine if they are suitable for military ground vehicle use. Several technologies were found to perform better than the state of the art compressed gas storage, exemplifying that advanced hydrogen storage could enable the electrification of the heaviest ground vehicles in the Army's fleet.

Citation: B. Paczkowski, A. Wiegand, "Model-Based Optimization of Hydrogen Storage for Military Ground Vehicle Applications," In *Proceedings of the Ground Vehicle Systems Engineering and Technology Symposium (GVSETS)*, NDIA, Novi, MI, Aug. 16-18, 2022.

1. INTRODUCTION

The Army has identified climate change as a significant threat, increasing the difficulty of the Army's core mission. In order to face the threat posed by climate change, the Army has planned several lines of effort including the fielding of fully electric tactical vehicles by 2050 [1]. Battery technology has matured significantly in recent decades and has clear potential for tactical vehicle electrification

efforts. However, battery energy density and fast charging rates make purely battery electric tactical vehicles a challenge. A potential solution to these challenges is hydrogen fuel cell power systems. Hydrogen fuel cells have the potential to provide longer range operation with less downtime than batteries. However, hydrogen is not without its difficulties, namely poor volumetric energy density at ambient conditions. Many hydrogen storage methods have been studied over the past decade, but there has not been an in-depth study on how certain methods would fit into military vehicle applications.

Military vehicles are also undergoing a drastic change in the way vehicle power is demanded and used. High power sensor suites are becoming more prevalent. Advances in technology are enabling new operating concepts. Developments in military doctrine are demanding more from a vehicle's power system than ever before. The US Army Training and Doctrine Command (TRADOC) has outlined several strategies in the U.S. Army Robotic and Autonomous Systems Strategy [2]. Concepts such as silent watch, where a vehicle shuts off its main engine but continues to provide power for communications equipment and sensors, and silent mobility, where a vehicle's main engine is shut down and the vehicle continues to move using a silent powertrain, require significant amounts of stored energy onboard a vehicle. Further developments in military technology, such as directed energy weapons systems, are also demanding large amounts of energy to be stored on vehicles in order to be deployed. The military is also interested in robotic and autonomy kits for vehicles, which require significant power and energy to operate effectively. It is difficult to meet these energy demands with current technology.

A potential solution to problems faced by both commercial and military vehicles is the hydrogen fuel cell. Commercially, hydrogen is of interest due to the potentially reduced environmental impact of the fuel. Hydrogen can potentially be produced from sustainable and non-carbon emitting sources by means of water electrolysis, among other technologies. However, electrolysis is an energy intensive process. The source of energy for electrolysis must be a carbon free source such as wind or solar in order for hydrogen to be a truly sustainable fuel. Hydrogen vehicles can also be refueled faster than battery electric vehicles, much like gasoline vehicles.

Hydrogen is of military interest due to the quieter and cooler operation compared to

internal combustion engines. Proton exchange membrane (PEM) fuel cells, a common fuel cell type used in automotive applications, operate at around 80°C [3]. This is a significantly lower temperature than diesel engines typically used in military vehicles, reducing the thermal signature immensely. PEM fuel cells also operate very quietly due to a lack of moving parts. The only audible sound emitted from a fuel cell vehicle when stationary is the fan noise from the air blower and cooling fans. Advantageous as it may be, hydrogen is not without flaws. In the gas phase, it has a very poor energy density. Storing hydrogen as a compressed gas requires lightweight but difficult to package cylindrical pressure vessels usually constructed from expensive carbon fiber. Compressed gas is not the only way to store hydrogen on vehicles. There are several technologies that have been developed to store hydrogen in a more effective way. Most of these have been investigated in passenger vehicle applications, not heavy duty applications that would be more relevant to military vehicles. Survivability concerns are also often raised in regard to storing hydrogen onboard military vehicles, though preliminary research and testing has shown that compressed hydrogen storage vessels are no more dangerous than liquid fuel storage tanks [4].

2. Scope

A select group of vehicles and hydrogen storage methods and materials were investigated for this analysis. The vehicles included are the M1280 Joint Light Tactical Vehicle (JLTV), M1085 Long Wheelbase Medium Tactical Vehicle (LWB MTV), M1075 Palletized Load System (PLS), M113 armored personnel carrier, Mobile Protected Firepower prototype (MPF), and M88 Recovery Vehicle. These vehicles were selected for a variety of weight ranges for both wheeled and tracked vehicles. The weights range from the 10,000 kg class to

above 50,000 kg in roughly 10,000 kg steps to provide a broad range of data. All other military vehicles are outside the scope of this work.

The hydrogen storage methods and materials included in this analysis are 350 and 700 bar compressed gaseous hydrogen, liquid hydrogen, cryo-compressed hydrogen, aluminum hydride (alane), magnesium nanoparticles encapsulated in reduced graphene oxide (rGO-Mg), metal organic framework 5 (MOF 5), methylcyclohexane (MCH)/toluene liquid organic hydrogen carrier (LOHC).

In the cases of cryogenic storage systems, dormancy (the duration of time the storage system can contain hydrogen in a cryogenic state before some boils off as a gas), heat transfer to the ambient, and ortho-para conversion (the conversion between electronic spin states of the individual hydrogen atoms in the diatom) will not be considered. Simple pipe flow and heat exchanger designs are used in this work for the purpose of identifying possible bottlenecks in vehicle design. More details models are outside the scope of work and should be used for specific system investigations when more parameters are known. Only the reaction from MCH to toluene will be considered in this work. Off-board processing of toluene into MCH is outside of the scope. Filling of MCH will only account for the flow of MCH into the vehicle and will not include the removal of toluene from the vehicle at the same time. All other hydrogen storage methods and materials are outside the scope of this project. Each analysis is performed with two load profiles: Churchville (cross country, mud, dust, and gravel surfaces) and Munson (primary road, paved and improved gravel surfaces). The profiles are based on courses at Army Testing and Evaluation Command (ATEC). All other load profiles are outside of the scope of work. A fuel cell hybridized with

a battery is used as a “drop in” replacement for the engine. A simple hybrid control strategy is used to control if the power comes from the fuel cell or the battery. For each simulation in this work, the strategy was set to sustain the charge of the battery in order to maximize the usage of the fuel cell. Regenerative braking was also simulated to recapture some of the vehicle’s energy while braking. Optimization of the hybrid architecture and the controls system is outside of the scope of work. Selection and performance of electric machines (e.g. motors) will be assumed, optimizing drivetrain performance is outside the scope. The packaging of the storage system including the dimensions, design, and protection against threat (survivability) is outside the scope of work.

3. Assumptions and Methodology

3.1. Vehicle Model

In order to streamline the vehicle simulation, several assumptions are made for certain parameters and components. A single fuel cell polarization curve is used for all of the vehicles simulated. This polarization curve is used as a single cell’s performance characteristics. The single cell is then connected in series to build a stack of sufficient power for the given application [5]. The fuel cell performance data used in the model is proprietary and unable to be disclosed. A single active area is assumed for this cell. The vehicles are modeled as fuel cell battery hybrid electric vehicles with the same amount of power available onboard as the conventionally fueled counterparts. The battery for vehicles was sized based on the kinetic energy of deceleration of the vehicle mass from 70 to 0 miles per hour [6].

The properties of the hydrogen storage materials investigated were selected at the same temperature and pressure when possible. These conditions are assumed to be close to the operation conditions that would be seen during normal operation.

The vehicle model was made and manipulated using Siemens LMS Amesim. Amesim is used to simulate the behavior of a vehicle operating over a variety of load profiles. Amesim is a simulation tool that uses validated component models, called submodels, to model complex engineering systems, such as vehicles. For each vehicle, a one dimensional model was built that accounted for the speed, grade, rolling resistance, cooling load, drag, and fuel consumption. The fundamental equation used to model vehicle road load is described in equation 1.

$$Load = f_r mg \cos\theta + \frac{1}{2} \rho_{air} c_d A v^2 + mg \sin\theta \quad (1)$$

The first term describes rolling resistance as a function of the friction on the surface, vehicle mass, gravitational constant, and cosine of the grade. The second term describes wind resistance as a function of the density of air, coefficient of drag, frontal area of the vehicle, and the square of the velocity. The final term describes the resistance due to a grade as a function of mass, gravity, and the sine of the grade. The model also includes several assumptions for vehicle performance that are described in reference [6]. The propulsion system is a fuel cell battery hybrid. The control strategy used in the model is battery charge sustaining based on the speed of the vehicle and distance traveled. For ease of analysis, vehicles are assumed to be weight neutral after the conversion to a fuel cell powertrain. This is a simplified approach and mass could vary significantly between a combustion engine and fuel cell vehicle. Future work will investigate the impacts of this assumption on the simulated results.

The size of the fuel cell stack is calculated based on maximum vehicle power calculated by the model. The model includes performance characteristics for an 80 kW fuel cell stack, which is scaled in integer steps depending on how much power the vehicle

requires. Certain vehicles require more than 80 kW, so multiples of the stack are used in the simulation. As the demanded power is calculated, the polarization and fuel consumption curves are used to calculate the amount of hydrogen consumed at that point in time. This fuel consumption is output and compared to the hydrogen storage material properties.

3.2. Hydrogen Storage

The material properties of the hydrogen storage technologies of interest were compiled from literature sources and physical property databases. When needed, the conditions (temperature and pressure) at which the property was measured is listed alongside the property.

Gaseous hydrogen is used onboard vehicles at two standardized pressures: 350 and 700 bar (approximately 5,000 and 10,000 psi, respectively). There are two types of pressure vessel commonly used, Type III and Type IV. Type III vessels are composed of a metal liner and carbon fiber overwrap and more frequently used in 350 bar applications. Type IV vessels contain a composite liner (usually high density polyethylene) and a carbon fiber overwrap. When considering pressure vessels, the key parameters are gravimetric and volumetric densities. Type IV vessels usually have a lower mass due to the composite liner and therefore a better gravimetric storage density. Type III vessels tend to be heavier but use less carbon fiber on the outside, improving the volumetric storage density. Another key parameter of gaseous hydrogen use is the flow rate of hydrogen from the storage vessel to the fuel cell. The gas flow submodels in Amesim were used to simulate the flow of hydrogen through a pressure regulator and stainless steel tubing typically used in vehicle applications.

Liquid hydrogen is a very high density form of hydrogen storage, storing the hydrogen in a liquid state at cryogenic temperatures. Cryo-compressed hydrogen is even denser

than liquid, as the liquid hydrogen is compressed to an elevated pressure (500 bar for this study). In order for the hydrogen to be usable in a fuel cell, it needs to be evaporated and heated to the operating temperature of the fuel cell. In order to achieve this, a heat exchanger was modeled, along with liquid and gaseous flow.

The materials for consideration in this section are solid state materials that store hydrogen via some sort of physical interaction, such as physisorption or chemical bonding, not actually hydrogen in a solid state. In order to link the flow rate of hydrogen needed by the fuel cell, several key parameters are needed. The reaction rate of the material is required to determine how quickly the hydrogen's bond to the material is broken. In most cases, heat is required to release the hydrogen. In order to accurately model this, heat capacity of the material needs to be known. Several sources were used to identify these properties at the operating conditions of the materials. In order to model the energy required to heat the material, equation 2 is used, where Q is the energy required to heat a block of mass m with the heat capacity c_p from a starting temperature to the temperature required to release all of the hydrogen stored, ΔT .

$$Q = mc_p\Delta T \quad (2)$$

The heater energy calculation assumes a perfectly insulated vessel with no heat loss to the outside and a uniform heating of the material. This energy is input into the model using the power offload provision built into the model. This is a simplified approach and will vary according to real world results, as some materials have a variable thermal conductivity with respect to hydrogen content. Alane is a well-documented example of this, with the thermal conductivity ranging from 0.915 W/mK when full of hydrogen to 18.2 W/mK when depleted of hydrogen [7].

Liquid organic hydrogen carriers (LOHC) store hydrogen bonded to a liquid organic material, such as methylcyclohexane (MCH) and toluene as considered in this work. MCH is fully hydrogenated (saturated), allowing hydrogen to be moved as a liquid. A catalyst is used to strip the hydrogen from MCH and convert it into toluene. The catalyst used for the dehydrogenation behavior of MCH in this work is 1 wt% Pt/ γ -Al₂O₃ as described by Usman et al [8]. The hydrogen is used in a fuel cell and the toluene is shipped back to a processing plant and reacted with a catalyst to saturate it again into MCH. Modeling this process requires the kinetics of the reaction, allowing for the release rate of hydrogen from MCH to be quantified.

All of the parameters used for these four materials are material-level properties. They are not system-level properties and as such do not account for any containment, heating devices, safety devices, and other balance of plant. Real world applications of such materials will have lower performance than indicated in this report. How much the properties shift from materials properties will be decided by system design and should be minimized by intelligent design processes.

3.3. Kinetic Models

Each material operates under different principles. As such, each has a unique kinetic model associated with it. All of these models have been retrieved from a review of the literature. Studies of rGO-Mg have revealed that the material has kinetics that are best described by the Johnson-Mehl-Avrami (JMA) model [9]. This model was used to calculate the flow rate of hydrogen as it is both desorbed from the material and absorbed when refilling. Alane can only be dehydrogenated due to extremely high pressures required for rehydrogenation [10]. Alane dehydrogenation has been found to follow the Avrami-Erofeyev model for decomposition, described in [11]. The kinetics of MOF-5 are mostly driven by the

diffusion of hydrogen into the pores of the material. It was found that a classic micropore diffusion model best describes the behavior of the material at several temperatures and pressures, shown in [12]. The overall mass of the material for each application was used to calculate the mass of hydrogen evolved or adsorbed and the derivative with respect to time was taken to calculate the mass flow rate of hydrogen. The adsorption and desorption isotherms have been demonstrated to be nearly identical, so the adsorption behavior was also used to describe the desorption behavior of MOF-5 [12]. The maximum hydrogen uptake was assumed to be 7.8 wt% [13]. Methylcyclohexane (MCH) dehydrogenation to toluene requires a catalyst and the exact kinetic behavior can vary depending on which catalyst is used. For this work, a kinetic model developed for a 1 wt% Pt/ γ -Al₂O₃ catalyst was used [8]. It was found that the Langmuir-Hinshelwood-Hougen-Watson (LHHW) kinetic theory best describes the behavior over this particular platinum catalyst. The model that offered the best fit involved the loss of the first hydrogen molecule as the rate limiting step [8].

3.4. Physical Models and Simulations

In order to determine the suitability of each technology for the various vehicle applications, the hydraulic and pneumatic libraries of Amesim were employed in several simple component models. These models and simulations allowed for design parameters to be tested, such as pipe diameters and flow rates. The pneumatic library in Amesim was used to model the flow of hydrogen gas through the plumbing onboard a vehicle. The real gas hydrogen submodel was used to simulate the behavior of hydrogen gas at 20°C flowing through a pipe to the fuel cell. The submodel uses the van der Waals equation of state to account for variations in behavior due to the non-ideal nature of the gas. The simulation was

performed with the mass flow rate set to each vehicle's peak hydrogen flow rate as determined by the vehicle model. The inner diameter of the pipe was varied to determine the minimum value that still allowed for full flow through the pipe. This was determined to be ½". A length of 3 meters was assumed for the pipe. The simulation accounts for friction through the pipe, but does not account for restrictions due to bends, pressure regulators and safety devices, and flow through the fuel cell. This model was used to simulate the flow of gas for the 350 bar and 700 bar gaseous hydrogen systems and the flow of gas after the heat exchanger for liquid and cryo-compressed hydrogen.

Amesim's hydraulic library was used to simulate the flow of both liquid hydrogen and MCH onto the vehicle in order to determine if each technology can refill a vehicle at a comparable rate to the current liquid fuel or 700 bar hydrogen. Each model used a constant volumetric flow source connected to a large chamber via a hose. The liquid hydrogen simulation does not account for environmental heat transfer losses and hydrogen losses due to precooling of the hose and nozzle before filling. Both of these effects warrant further investigation but are outside the scope of this work.

Design equations for a shell and tube heat exchanger were used to determine if the heat exchanger would cause any flow restrictions for the liquid hydrogen and cryo-compressed hydrogen systems. A heat exchanger with water at ambient conditions as the working fluid was designed to vaporize and heat the hydrogen to ambient conditions. The design equations used can be found in [14]. The design does not account for the freezing of the process fluid and temperatures were selected to avoid this phenomenon. Two phase flow was not included in the design calculations.

4. Results and Discussion

4.1. Vehicle Modeling

Vehicle parameters including weight, frontal area, drag coefficient, and rolling resistance were input into the Amesim model. Vehicles are listed in order of ascending weight with the first three vehicles being wheeled vehicles and the final three tracked vehicles. The first simulation was run to determine how much hydrogen is required onboard each vehicle to meet the required range in Table 1. In order to determine this, the vehicles were set to a constant speed, shown in Table 1. The road conditions were set to a 0% grade paved road 10 miles long. In order to simulate the worst case scenario, the battery control was set to sustain the battery charge. This forces the fuel cell to either provide the power to propel the vehicle or immediately recharge the battery after it has been discharged and thus maximizes the hydrogen consumption. The hydrogen consumption and fuel economy were calculated utilizing the post-processing capability of Amesim. The required range was divided by the fuel economy to provide the required amount of hydrogen storage for each vehicle.

Table 1: Simulation results for the hydrogen storage capacity determination.

Vehicle	Speed (mph)	Economy (mi/kg)	Required Range (mi)	Required H ₂ Storage (kg)
M1280	35	23.2	300	12.9
M1085	35	10.6	300	28.4
M1075	35	6.7	300	44.7
M113	25	3.8	300	78
MPF	25	3.3	300	91
M88A1	20	0.88	280	318.9

As expected, the amount of hydrogen required onboard increases with vehicle weight. Lighter vehicles achieve better fuel economy and utilize less power, requiring less fuel to meet the range target. There is also a noticeable increase in power and fuel needs for tracked vehicles compared to

wheeled vehicles. This could be due to the varying frontal area, as the tracked vehicles have a much more box-like profile than the wheeled vehicles, and the increased rolling resistance of the track. The required amount of hydrogen stored on board the vehicle is used in later calculations to determine several storage system parameters, such as overall mass and volume and heater power requirements.

In addition to the flat 10 mile simulation, two courses were simulated: Munson, a primary road with a single hill, and Churchville, and aggressive cross country course. For each course, the maximum power that the battery could accept from regenerative braking was set to 120 kW and the battery control strategy was charge sustaining. The target speed for Munson was 25 miles per hour for each vehicle. Table 2 summarizes the results of the Munson simulation for each vehicle.

Table 2: Munson course simulation results

Vehicle	Average Speed (mph)	Economy (mi/kg)	Maximum Consumption (g/s)
M1280	25.3	27.2	0.4
M1085	25.3	11.1	2.8
M1075	25.3	5.0	5.5
M113	24.5	4.3	2.6
MPF	24.6	3.6	2.8
M88	24.3	0.8	10.6

As with the flat course, the hydrogen consumption increases for the heavier vehicles. The tracked vehicles appeared to struggle to meet the speed threshold for the course, as all three are below the 25 mile per hour target. The fuel economy is the same order of magnitude as the flat course with some minor difference between the two runs.

The Churchville profile is based on a very aggressive off-road cross-country course. The target speed for each vehicle was 15 miles per hour. The results of the simulation are listed in Table 3.

The aggressive nature of the course is apparent, as none of the vehicles can maintain the target speed over the course. Hydrogen economy dropped significantly compared to both the flat course and Munson, decreasing by an order of magnitude in some cases. The hydrogen consumption is also higher across the board. The maximum consumption from this run will be used as the hydrogen consumption for the kinetic models as it is the most aggressive the vehicles will potentially experience.

Table 3: Churchville simulation results.

Vehicle	Average Speed (mph)	Economy (mi/kg)	Maximum Consumption (g/s)
M1280	14.3	4.2	1.4
M1085	14.2	1.5	3.4
M1075	14.2	0.8	6.2
M113	14.1	2.0	3.1
MPF	14.1	1.5	4.3
M88	14.5	0.6	11.8

4.2. Hydrogen Storage Material Properties

In order to thoroughly analyze the performance of each hydrogen storage method, the relevant material properties for each method were gathered from literature sources. Table 5 lists the properties used in this work.

4.3. Hydrogen Storage Applications for Modeled Systems

Based on the results of the first simulation shown in Table 1, the mass of each system for each vehicle was calculated. The required amount of hydrogen was divided by the gravimetric capacity of the system to provide the overall system mass, shown in Table 4.

There are several interesting trends to note in this analysis. The first is that the heaviest storage technology is 700 bar compressed gas, which is widely considered to be the most mature hydrogen storage technology. Even with material advances, the sheer amount of carbon fiber required to safely

store such high pressure hydrogen is still significant. High safety margins are required and long service life is expected, driving the need for bulky systems. A potential compromise is 350 bar compressed hydrogen, which requires less material due to the lower pressure. However, the loss of capacity due to the lower pressure while remaining the second heaviest system make its use difficult to justify.

On the opposite end of the spectrum, cryo-compressed hydrogen (CcH2) is consistently the lightest weight storage method for vehicles. CcH2 involves the storage of hydrogen at cryogenic temperatures and elevated pressures, usually around 60 K or below and 500 bar [24]. Storing the hydrogen at elevated pressures significantly reduces the boil-off of hydrogen compared to liquid [23]. Storing the hydrogen in a compressed state at cryogenic temperatures reduces the frequency of hydrogen gas purges because the system is designed to handle pressure. This is not the case with conventional liquid storage, which is designed to hold an unpressurized cryogenic liquid.

Method	M1280	M1085	M1075	M113	MPF	M88
350 bar	239	526	828	1444	1685	5906
700 bar	307	676	1064	1857	2167	7593
Liquid	163	359	566	987	1152	4037
CcH2	117	258	406	709	827	2899
rGO-Mg	198	437	688	1200	1400	4906
Alane	128	281	443	772	901	3157
MOF-5	165	364	573	1000	1167	4088
MCH	208	458	721	1258	1468	5144

Table 4: The mass of the hydrogen storage system for each vehicle in kilograms.

The increased density of hydrogen in its liquid state allows for significantly more to be stored onboard while the low pressure operation requires less material than compressed gas. There is a requirement for insulation and heat exchangers, which slightly increase the weight compared to CcH2. There is one significant drawback with liquid hydrogen storage: boil-off. Boil-off is the release of hydrogen from the ullage (gaseous layer above the liquid) to maintain operating pressure in the vessel as hydrogen boils due to an external heat input. There are two main causes for boil-off: heat from the environment and ortho-para conversion, a process in which the spin states of the hydrogen atoms change from ortho-hydrogen to para-hydrogen, releasing heat [30]. The resulting gas has the potential to exceed the pressure rating of the vessel. To avoid this, the gas is released from the vessel once a certain pressure threshold has been met. If a vehicle sits dormant for an extended period of time, the potential exists to lose a significant amount of hydrogen to boil-off, reducing the ability for vehicles to be ready for use at a moment's notice. The release of hydrogen from vehicles also introduces a challenge in storing the vehicles when not in use. The vehicles will need to be stored in a well ventilated area that will not allow for the accumulation of hydrogen due to the wide flammability range of the gas [31].

Another concern that is applicable to both liquid and CcH2 is the energy cost of liquefaction. Hydrogen has a very low

boiling point of 22 K, requiring significant energy to reach. About 40% of the higher heating value of hydrogen is required to liquefy hydrogen with current technologies [20]. This energy cost is not borne by the vehicle but rather an external cost paid at the or before the fueling point, so there is no impact in range due to this energy requirement. This is a significant area for improvement and there are some technologies being developed to reduce the energy input for hydrogen liquefaction, such as magnetocaloric liquefaction [32].

Of the less conventional hydrogen storage materials, alane has the lowest weight followed by MOF-5. Both are slightly heavier than CcH2, yet significantly lighter than both compressed gas systems. This is encouraging, as alane is a stable hydrogen storage medium that can allow for long-term storage of vehicles. The drawback for alane is that it is a single use material, much like a primary battery. The hydrogen can be easily released from the material onboard a vehicle by heating, but it cannot be easily recharged onboard a vehicle due to extremely high pressure requirements [10]. In order to refill the vehicles with alane, solid block(s) will need to be unloaded and reloaded, which could become a time consuming process. Depending on the vehicle, significant amounts of alane are required, ranging from 100 kg to over 1,500 kg. Smaller amounts could be man-lifted onto the vehicle by several people, but larger amounts will

Table 5: Hydrogen storage material properties.

Technology	Gravimetric (wt%)	Volumetric (kg H ₂ /L)	Uptake rate (g H ₂ /s)	Heat capacity (J/mol K)	Operating conditions
350 bar compressed	5.4 [15]	0.018 [15]	120 [16]	21.078 [17]	350 bar, atmospheric temp [16]
700 bar compressed	4.2 [18]	0.024 [18]	60 [19]	21.568 [17]	700 bar, atmospheric temp [18]
Liquid	7.9 [20]	0.035 [20]	27.7 [21]	19.7 [17]	22 K, 150 psig [21] [22]
Cryo-compressed	7.8- 11 [23]	0.0745 [23]	25.8 [22]	14.897 [17]	500 bar, 60 K [24]
rGO-Mg	6.5 [25]	0.105 [9]	8.9-220.5	35.4	250-350°C, 15 bar H ₂ [9]
Alane	10.1 [26]	0.15 [26]	N/A	40.2 [7]	150°C, atmospheric pressure [7]
MOF-5	7.8 [13]	0.052 [13]	784	0.25 [27]	77 K, 40 bar [13]
MCH	6.2 [28]	0.047 [28]	30.4	185 [29]	200-300°C, 10-50 bar [28]

require material handling equipment, which is concerning.

For the materials requiring heat to release the hydrogen (rGO-Mg, alane, MOF-5, and MCH), the energy required to heat the materials to a sufficient temperature to release the hydrogen required for each vehicle was calculated. The energy required was then compared to the lower heating value of hydrogen to determine the percentage of hydrogen stored within the material used for the purpose of heating the material. MOF-5 utilizes only 0.6% of the hydrogen stored, while alane uses 1.4%, rGO-Mg uses 5.6%, and MCH uses 6.97%. In each case, the range of the vehicle will be impacted by this requirement because the percentage of hydrogen listed above will be utilized to heat the material rather than propel the vehicle, effectively reducing the amount of hydrogen stored in the system. To account for this, the amount of hydrogen stored on board will need to be increased. This leads to a recursive relationship, as increasing the amount of hydrogen stored will increase the mass of the system and therefore the vehicle, potentially requiring more fuel to meet the required range. This impact is outside the scope of this work but will be critical to understand as research into alternative propulsion continues.

4.4. Kinetic Models

Two kinetic models were run for rGO-Mg, one for hydrogen absorption and one for hydrogen desorption. Both simulations were run for a duration of 10 minutes. Absorption was modeled at a constant temperature of 250°C and the average uptake rate over the simulation time was calculated. In order to meet the current state of the art performance of 700 bar compressed hydrogen, a fill rate of 60 grams per second is required. Only the MPF and M88 were able to maintain such a high flow rate over 10 minutes, all of the other vehicles did not meet this threshold. This kinetic barrier is a known issue with this

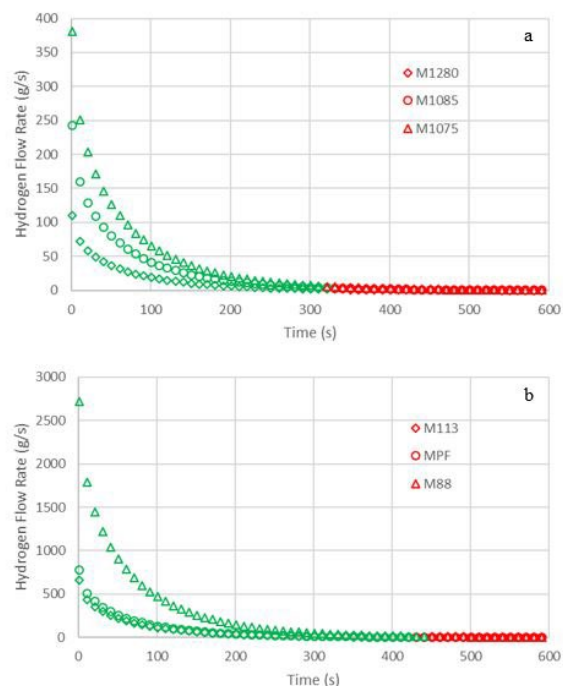


Figure 1: Hydrogen flow rates from rGO-Mg for wheeled (a) and tracked (b) vehicles.

material. In order to improve the absorption rate, doping with nickel has been investigated [25]. Doping does improve the uptake rate but reduces the overall hydrogen capacity. A trade off study in order to determine if the doped material meets the requirements is needed.

On the other hand, desorption was modeled at a constant temperature of 350°C. For clarity, the wheeled and tracked vehicles were separated into different plots. Figure 1a shows the flow rate of hydrogen for the wheeled vehicles and Figure 1b shows the tracked vehicles. The plots are colored to show when the flow rate drops below the target flow rate for that specific vehicle. Data points in green are above or equal to the target flow rate and red points are below the target flow rate.

The wheeled vehicles show flow rates well in excess of the target value with an exponential decay trend. The flow of hydrogen meets or exceeds the target value for approximately 5 minutes for each vehicle before dropping below the target. Due to the

way the model was run, the material is assumed to be at the operating temperature at the beginning of hydrogen flow. As such, the maximum flow rate is observed at the start of the simulation. The same trend can be observed for the tracked vehicles. They all maintain a high hydrogen flow rate initially, eventually tailing off. However, the tracked vehicles are able to maintain flow above the target for longer than the wheeled vehicles, tailing off at approximately 7.5 minutes. Due to the large amount of material present, the initial flow rate is significantly higher than the target value. The flows are more than sufficient to meet the needs for peak power. The control system will need to be carefully designed such that the flow can be maintained for a long duration while also allowing for peak flow to be reached. Transient response should also be investigated with the thermal conductivity of the material taken into account.

Due to the irreversible nature of alane, only the dehydrogenation kinetics were modeled. Dehydrogenation has an onset temperature of approximately 60°C, with peak flow taking place at 138°C [11]. This peak temperature was used for the kinetic model. As with the previous material, the vehicles were split between wheeled and tracked to provide clarity. The model was run for 60 seconds. Figure 2a shows the results for the wheeled vehicles and Figure 2b shows the tracked vehicles.

Unlike rGO-Mg, alane does not immediately release hydrogen at its maximum flow rate. This is consistent with the induction period observed by Graetz et al, where decomposition is slower at low levels of fractional decomposition [11]. There is a slight lag in the release of hydrogen for each vehicle as the material begins to decompose and hydrogen release sites begin to form. The delay is longest for the wheeled vehicles and approximately three times shorter for the tracked vehicles. A lag in hydrogen release is

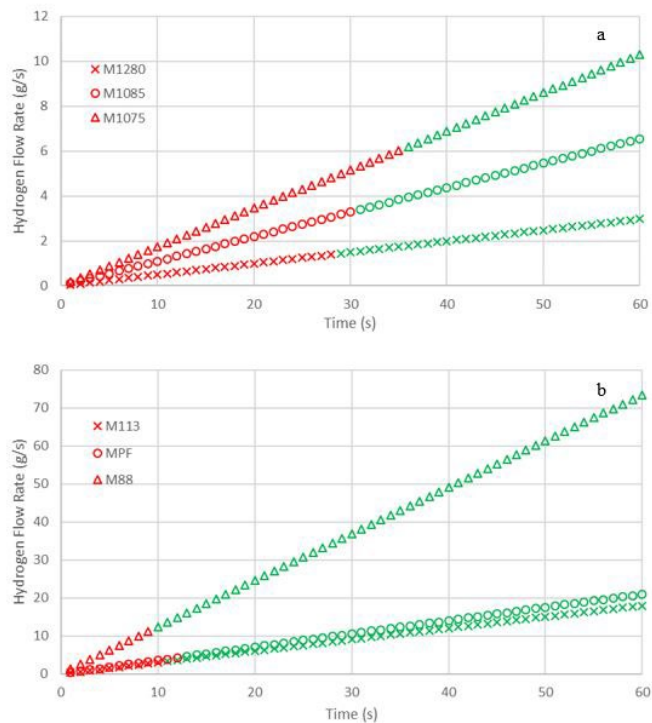


Figure 2: Hydrogen flow rates from alane for wheeled (a) and tracked (b) vehicles.

not a desirable trait, but the model demonstrates that the required flow rates are met within a relatively short period of time. There are potential engineering strategies that can be used to compensate for the delayed time to full flow, such as setting battery limits to ensure that there is enough energy stored at a given time to meet the most strenuous conditions for the time required to reach full hydrogen flow. Transient modeling would allow for a better understanding of the material's behavior and should be developed.

The adsorption behavior of MOF-5 was modeled and found to be incredibly fast. The average flow rate over 10 seconds was at least an order of magnitude higher than the required 60 g/s described previously. The flow into the material ranged from 784 g/s for the M1280 to 19,386 g/s for the M88. The highly porous structure of MOF-5 facilitates hydrogen diffusion, providing incredibly fast kinetics. The hydrogen release is equally as impressive. Figure 3a shows the behavior for

the wheeled vehicles and Figure 3b shows the behavior for the tracked vehicles.

The desorption behavior of MOF-5 is also sufficient for each use case investigated. When operating as modeled, at full capacity, the initial flow rates are incredibly high. The hydrogen is readily desorbed in massive quantities and can be completely discharged in a matter of seconds. The flow rates from MOF-5 are the highest of any material, which can be advantageous in quick start scenarios. However, if allowed to operate as modeled, significant challenges will arise. The flow of hydrogen will cause thermal issues, releasing heat that will need to be mitigated. The massive amount of hydrogen will not be completely utilized by the fuel cell and could potentially cause an overpressurization of the system. Even if the fuel cell system is equipped with hydrogen recirculation, it will most likely be unable to handle such a large amount of hydrogen so quickly. In extreme conditions, this could cause hydrogen to be lost to the environment. However, the flow rate could be tailored to meet fuel cell demand since the system operates primarily through pressure swings. The uptake rate can also be controlled by regulating the pressure of the hydrogen flowing into the material. A well-engineered system that accounts for the thermal needs and tightly controls hydrogen flow could harness the incredible kinetics of MOF-5 and allow for near-instant hydrogen flow source that follows the demands of the fuel cell.

The kinetics of MCH are controlled primarily by the catalyst loading and the deactivation time of the catalyst. The amount of catalyst was varied and the amount of catalyst required to meet the target flow rate of hydrogen for each vehicle was recorded. The catalyst deactivation time was set to 5 days, allowing for vehicles to operate at full flow for 5 days straight. After 5 days, the catalyst will need to be regenerated by flowing hydrogen over the catalyst as it is

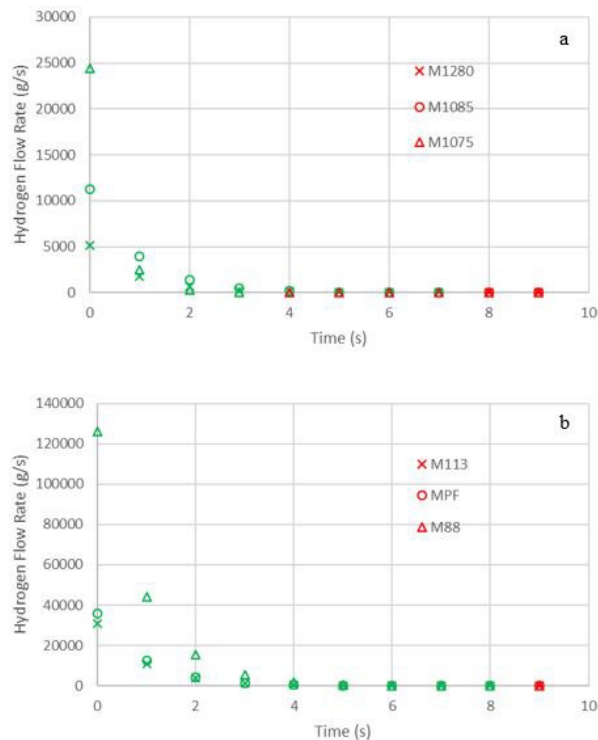


Figure 3: Hydrogen flow rates from MOF-5 for wheeled (a) and tracked (b) vehicles.

heated. A future investigation into the accepted duration for consumable parts should be done to validate this assumption and correct the results, if needed.

The model validates that MCH can be dehydrogenated at a fast enough rate to provide hydrogen to each vehicle under the most demanding conditions. The amount of catalyst required increases with the rate, shown in Table 6. The mass of the catalyst is not insignificant, varying between 5 and 19 percent of the mass of liquid needed to meet the required range. Similar to the energy requirements for the heater, the added mass of the catalyst will reduce the gravimetric density of the overall system, reducing performance. Accounting for the weight of the catalyst, the gravimetric density for MCH is reduced from 6.2 weight percent to between 5.2 and 5.9 weight percent. This still surpasses 700 bar compressed hydrogen but reduces the margin for any other components required to support the system, such as the

reactor vessel. MCH may also require hydrogen purification after the dehydrogenation step, as the hydrogen may not meet the purity standards for fuel cell use. This will add mass and complexity to the system.

Table 6: Catalyst loading required to meet the target hydrogen flow rate for each vehicle.

Vehicle	Catalyst Loading (kg)	Percentage of system mass
M1280	32	15
M1085	75	16
M1075	138	19
M113	68	5
MPF	97	7
M88	264	5

4.5. Physical Simulations

In order to investigate if the plumbing from the hydrogen storage system to the fuel cell would cause any losses in flow, a gas flow system was modeled for each vehicle. The results for this simulation can be applied to all of the systems after the materials have undergone reactions and/or conversion to gaseous hydrogen. The simulation results determined that the system, as designed, is able to meet the maximum flow rate for each vehicle. The plumbing of the system does not cause any losses in flow due to friction or turbulent flow effects at the steady state conditions simulated.

Two liquid systems were simulated, liquid hydrogen and MCH. Liquid hydrogen was set to a flow rate of 52 liters per minute, which is approximately the 60 g/s requirement for gaseous hydrogen at the density of liquid hydrogen. Flow was simulated over 10 minutes. The simulation determined that the system is able to maintain the flow of hydrogen, showing that there will be no bottlenecks in refueling caused by the plumbing. The flow rate is also significantly higher than the target flow rate needed by the

fuel cell for each vehicle so it can be determined that flow from the tank to the heat exchanger will not cause the flow to be reduced.

MCH flow was simulated at several different flow rates to simulate vehicles being refilled by different systems, assuming they were modified for MCH service. Flow rates of 40, 70, and 100 gallons per minute were simulated. Pumps currently used for private and commercial vehicle service are rated at 40 gallons per minute and the hose simulated is rated up to 70 gallons per minute [33]. Military fuel systems can fill up to 600 gallons per minute for transfer between storage vessels, but a flow of 100 gallons per minute was simulated to test if the simulated hose could handle higher than rated flow without reducing flow significantly or bursting [34].

The system is able to maintain flow at all three rates for 10 minutes without a significant reduction in flow and the hose is able to maintain a higher than rated flow rate. Less than 0.1% of the flow is lost through the pipes at all three flow rates. The simulated results show that the vehicles will be able to maintain fill time parity with the current liquid fuel when using MCH.

Both the liquid hydrogen and cryo-compressed hydrogen systems require a heat exchanger to vaporize the stored hydrogen to gaseous hydrogen to be used in the fuel cell. A simple preliminary design for two heat exchangers was performed to determine if it is possible to design a heat exchanger that meets the target flow rates without significant pressure drop or flow restrictions. The working fluid used was water. Table 7 shows the heat duties and heat transfer area for both cases.

The heat exchangers can handle the target flow rate for each vehicle. There was no loss of flow observed for any of the vehicles. The heat transfer area required for each vehicle increases with the flow rate. Nearly a square

meter is required for the cryo-compressed system on the M88. Depending on how the heat exchanger is packaged, this will take up a significant volume. Overall, the liquid hydrogen systems require a heat exchanger with a smaller heat transfer area than the cryo-compressed systems. This is most likely due to the larger temperature difference between the hydrogen and the working fluid, which is nearly 40 K higher than the cryo-compressed system. However, due to this higher temperature difference, the heat duty of the working fluid is higher for liquid hydrogen than it is for cryo-compressed. The heat duty of each system is significant. More components to the system will be required, such as a heater for the working fluid or a secondary heat exchanger between either the ambient air or the fuel cell cooling loop. A detailed design study will be needed to understand the complete demands of the system. This preliminary design has validated that it is possible to design a heat exchanger for the target flow rates without a significant pressure drop or flow restrictions.

Table 7: Heat exchanger design parameters for liquid and cryo-compressed hydrogen.

Vehicle	Liquid Hydrogen		Cryo-compressed Hydrogen	
	Heat Duty (W)	Heat Transfer Area (m ²)	Heat Duty (W)	Heat Transfer Area (m ²)
M1280	3598	0.11	3359	0.11
M1085	8738	0.27	8157	0.28
M1075	15934	0.49	14874	0.51
M113	7967	0.24	7437	0.25
MPF	11051	0.34	10316	0.35
M88	30326	0.92	28308	0.96

5. Conclusion

This analysis has demonstrated that there are several technologies that can potentially outperform 700 bar compressed gas hydrogen storage, the current state of the art,

when applied to military vehicles. When optimized for mass, volume, and ability to sustain the maximum flow of hydrogen in demanding conditions, it was found that cryo-compressed hydrogen provides the best performance. Compared with 700 bar compressed hydrogen, cryo-compressed hydrogen can store 160% of the hydrogen per unit weight and 300% more hydrogen per liter. The use of cryo-compressed hydrogen in the place of 700 bar compressed gas has the potential to reduce the cost of the storage vessel by reducing the amount of carbon fiber needed [23]. Cryo-compressed hydrogen can be refilled at a similar speed to current fuels, maintaining current readiness levels.

Several other technologies are worth investigation and have the potential to be future hydrogen storage methods for military ground vehicles. MOF-5 has incredibly fast kinetics and higher gravimetric and volumetric storage densities than compressed hydrogen gas. If the gravimetric density can be maintained near room temperature, MOF-5 systems could be less complex than both compressed gas and cryo-compressed while providing similar performance. Alane is also of interest due to its high gravimetric and volumetric hydrogen densities, however there may be challenges with loading and unloading large amounts of the material onto vehicles. This lends it towards smaller vehicle use, where less material is needed.

The simulations also found that rGO-Mg and MCH are potentially unsuitable for military ground vehicle application. Both rGO-Mg and MCH require 5% or more of the energy of the stored hydrogen to be released. There is a challenge with rGO-Mg meeting the filling time requirements for the vehicles. The smaller vehicles are unable to uptake hydrogen at a rate near the current state of the art, which is problematic. MCH also requires a catalyst, which reduces the gravimetric storage capacity compared to the other technologies. There is a chance the hydrogen

coming from the MCH dehydrogenation reactor does not meet the purity requirements for hydrogen vehicles, requiring a purification step that will also add mass and volume to the system. The added challenge of storing two liquids onboard with an MCH system reduces its attractiveness. The toluene product from the dehydrogenation reaction will need to be stored onboard to be reprocessed offboard for future use. This added complexity is not present in the two leading technologies.

As military vehicles embrace electrification and its many benefits, this analysis shows that hydrogen fuel cells and advanced hydrogen storage technologies can play a role in future ground vehicle applications. While storing hydrogen as a compressed gas is the current state of the art, it is clear that other technologies are quickly advancing and show potential to outperform it. Based on the encouraging results of the simulations performed, continued research into the applications of cryo-compressed hydrogen, MOF-5, and alane for military ground vehicle applications is recommended.

6. REFERENCES

- [1] "Army Climate Strategy," 2022.
- [2] D. Allyn, "The U.S. Army Robotic and Autonomous System Strategy," U.S. Army TRADOC, Fort Eustis, 2017.
- [3] J. Zhang, T. Fisher, P. Ramachandran, J. Gore and I. Mudawar, "A Review of Heat Transfer Issues in Hydrogen Storage Technologies," *Journal of Heat Transfer*, pp. 1391-1399, 2005.
- [4] B. Paczkowski, "Ballistic Testing of Pressurized Hydrogen Storage Cylinders," in *Power Sources Conference*, Denver, 2018.
- [5] J. Larminie and A. Dicks, *Fuel Cell Systems Explained*, John Wiley & Sons, 2003.
- [6] A. Wiegand, "Fuel Economy Modeling of Army Fuel Cell Hybrid Vehicles, Part 1," Defence Technical Information Center, 2018.
- [7] R. Zidan, P. Ward, B. Hardy and S. McWhorter, "Investigation of Solid State Hydrides for Autonomous Fuel Cell Vehicles," US Department of Energy, Washington, D.C., 2017.
- [8] M. Usman, D. Cresswell and A. Garforth, "Detailed Reaction Kinetics for the Dehydrogenation of Methylcyclohexane over Pt Catalyst," *Industrial & Engineering Chemical Research*, vol. 51, pp. 158-170, 2001.
- [9] E. Cho, A. Ruminski, S. Aloni, Y.-S. Liu, J. Guo and J. Urban, "Graphene oxide/metal nanocrystal multilaminates as the atomic limit for safe and selective hydrogen storage," *Nature Communications*, pp. 1-8, 2016.
- [10] J. Graetz, J. Reilly, V. Yartys, J. Maehlen, B. Bulychev, V. Antonov, B. Tarasov and I. Gabis, "Aluminum hydride as a hydrogen and energy storage material: Past, present and future," *Journal of Alloys and Compounds*, vol. 509, no. S2, pp. S517-S528, 2010.
- [11] J. Graetz and J. J. Reilly, "Decomposition Kinetics of the AlH₃ Polymorphs," *Journal of Physical Chemistry*, pp. 22181-22185, 2005.
- [12] D. Saha, Z. Wei and S. Deng, "Hydrogen adsorption equilibrium and kinetics in metal-organic framework (MOF-5) synthesized with DEF approach," *Separation and Purification Technology*, vol. 64, pp. 280-287, 2008.

- [13] A. Ahmed, S. Kuthuru, D. Aulakh, J. Purewal, A. Wong-Foy, A. V. M. Matzger and D. Siegel, "Optimized Hydrogen Adsorbents via Machine Learning and Crystal Engineering," in *DOE Annual Merit Review*, Washington, D.C., 2019.
- [14] S. Ahmed, "ChE Resources Shell and Tube Heat Exchanger Design in MS Excel," 2013. [Online]. Available: <https://www.cheresources.com/invision/topic/19924-design-a-shell-tube-heat-exchanger-on-ms-excel/>. [Accessed 31 March 2020].
- [15] U. DRIVE, "Hydrogen Storage Tech Team Roadmap," 2017.
- [16] A. Elgowainy, "Hydrogen Refueling Analysis of Fuel Cell Heavy-Duty Vehicles Fleet," in *International H2 Infrastructure Workshop*, Boston, 2018.
- [17] NIST, "Thermophysical Properties of Hydrogen," 2020. [Online]. Available: <https://webbook.nist.gov/cgi/fluid.cgi?ID=C1333740&Action=Page%20>.
- [18] DOE, "Physical Hydrogen Storage," 2019.
- [19] SAE, "J2601: Fueling Protocols for Light Duty Gaseous Hydrogen Surface Vehicles," Society of Automotive Engineers, 2016.
- [20] J. Milliken, J. Petrovic and W. Podolski, "Hydrogen Storage Issues for Automotive Fuel Cells," in *International Workshop on Hydrogen in Materials and Vacuum Systems*, Newport News, 2002.
- [21] S. Aceves, G. Berry, F. Espinosa-Loza, G. Petitpas, V. Switzer and S. Tuholski, "LLNL/Linde 875 Liquid Hydrogen Pump for High Density Cryogenic Vessel Refueling," in *FY 2012 Annual Progress Report*, 2012.
- [22] G. Petitpas, A. Simon, J. Moreno-Blanco and S. M. Aceves, "Liquid Hydrogen Infrastructure Analysis," in *DOE Hydrogen and Fuel Cells Annual Merit Review*, Washington, D.C., 2018.
- [23] R. Ahluwalia, D. Papadias, J.-K. Peng and H. Roh, "System Level Analysis of Hydrogen Storage Options," in *2019 Annual Merit Review and Peer Evaluation Meeting*, Washington, D.C., 2019.
- [24] K. Kunze and O. Kircher, "Cryo-compressed Hydrogen Storage," in *Cryogenic Cluster Day*, Oxford, 2012.
- [25] E. Cho, A. Ruminsky, Y.-S. Liu, P. Shea, S. Kang, E. Zaia, J. Park, Y.-D. Chuang, J. Yuk, X. Zhou, T. Heo, J. Guo, B. Wood and J. Urban, "Hierarchically Controlled Inside-Out Doping of Mg Nanocomposites for Moderate Temperature Hydrogen Storage," *Advanced Functional Materials*, pp. 1-11, 2017.
- [26] J. Graetz, J. Reilly, G. Sandrock, J. Johnson, W. Zhou and J. Wegrzyn, "Aluminum Hydride, AlH₃, As a Hydrogen Storage Compound," Brookhaven National Laboratory, Upton, 2006.
- [27] F. Kloutse, R. Zacharia, D. Cossement and R. Chahine, "Specific heat capacities of MOF-5, Cu-BTC, Fe-BTC, MOF-177 and MIL-53 (Al) over wide temperature ranges: Measurements and application of empirical group contribution method," *Microporous and Mesoporous Materials*, pp. 1-5, 2015.
- [28] A. Wijayanta, T. Oda, C. Purnomo, T. Kashiwagi and M. Aziz, "Liquid hydrogen, methylcyclohexane, and ammonia as potential hydrogen storage: Comparison review,"

- International Journal of Hydrogen Energy*, pp. 15026-15044, 2019.
- [29] NIST, "NIST Chemistry WebBook," [Online]. Available: <https://webbook.nist.gov/cgi/cbook.cgi?ID=C108872&Mask=FFF>.
- [30] S. Gursu, M. Lordgooei, S. Sherif and T. Veziroglu, "An optimization study of liquid hydrogen boil-off losses," *International Journal of Hydrogen Energy*, vol. 17, no. 3, pp. 227-236, 1992.
- [31] "Lower and Upper Explosive Limits for Flammable Gases and Vapors (LEL/UEL)," [Online]. Available: [https://www.mathesongas.com/pdfs/products/Lower-\(LEL\)-&-Upper-\(UEL\)-Explosive-Limits-.pdf](https://www.mathesongas.com/pdfs/products/Lower-(LEL)-&-Upper-(UEL)-Explosive-Limits-.pdf). [Accessed 9 March 2020].
- [32] J. Holladay, "MagnetoCaloric Hydrogen Liquefaction," in *Department of Energy Annual Merit Review*, Washington, D.C., 2019.
- [33] "UL-Listed Low-Pressure Gasoline Hose," McMaster-Carr, [Online]. Available: <https://www.mcmaster.com/5396k54-5396K43>. [Accessed March 2020].
- [34] L. DRS, "Modular Fuel System," [Online]. Available: leonardodrs.com. [Accessed March 2020].